Journal of Thermal Analysis and Calorimetry (2022) 147:8535–8549
https://doi.org/10.1007/s10973-021-11138-x

Product distribution and coke formation during catalytic pyrolysis of oil shale with zeolites

Xiaoye Wang[1] · Yulong You[1] · Xiangxin Han[1] · Xiumin Jiang[1]

Received: 21 March 2021 / Accepted: 30 October 2021 / Published online: 1 December 2021

Abstract
Catalytic pyrolysis is useful for product regulation of fuel. In this work, we studied oil shale catalytic pyrolysis with HZSM-5 and HUSY by experiments and DFT calculation. We discussed the catalytic pyrolysis in detail by analyzing product distribution, coke characteristics and adsorption of hydrocarbons in zeolites. Catalytic cracking of long-chain aliphatics and formation of light aromatics increase light fraction in shale oil. Coke comes from growth of coke precursors and deposition of long-chain compounds. In comparison, catalytic pyrolysis with HZSM-5 has higher yield of hydrocarbon gases, less content of alkenes in shale oil and low coke yield, while catalytic pyrolysis with HUSY has high content of aromatics in shale oil and high coke yield. Product distribution is affected by zeolite characteristics and pyrolysis conditions. Pore size of zeolites affects the diffusion and conversion of compounds and formation of coke, which makes two zeolites show different shape-selective effects. Competition between alkanes, alkenes and aromatics for Brønsted acid and coke species deposited in zeolites was analyzed by DFT calculation. Increasing temperature from 490 to 520 ℃ significantly promotes cracking in catalytic pyrolysis with HZSM-5 and aromatization in catalytic pyrolysis with HUSY. This study indicates optimizing zeolite characteristics and catalytic pyrolysis condition could realize directional regulation of volatile products and improvement of quality of shale oil.

Keywords Oil shale · Catalytic pyrolysis · Zeolite · Coke · DFT

Introduction

Modern economic and industry development have increased energy demand. Oil shale has received many attention as an unconventional alternative energy source with huge reserves. Pyrolysis is widely used to convert oil shale to valuable shale oil and gas products. Shale oil is complex and has higher content of oxygen, nitrogen and sulfur compared to conventional crude oil, and meanwhile contains a certain amount of heavy fraction, which needs further processing for utilization [1, 2]. Therefore, the key of effective utilization of oil shale resource is improving yield and quality of shale oil and gas products.

Oil shale pyrolysis is affected by characteristics of kerogen and mineral composition [3], and pyrolysis conditions such as temperature [2], particle size [4], heating rate [5] and catalysis. Catalytic pyrolysis of fuels is carried out by adding catalysts or changing pyrolysis atmosphere to regulate pyrolysis processes and selectively increase yields of target products. Currently, catalysts of oil shale pyrolysis studied include shale ash, metal salt, zeolites and so on.

Catalytic pyrolysis with zeolite has been rapidly developed in recent years. Zeolites have various catalytic functions based on pore structure and acid property to realize the directional regulation of pyrolysis process. For example, abundant researches have shown that ZSM-5 can effectively achieve catalytic deoxygenation during biomass pyrolysis and selectively convert biomass into high value-added chemicals such as light olefins and aromatics [7–11]. Acid site in zeolite could effectively promote cracking process. Many researchers used zeolites for catalytic pyrolysis waste polyolefinic plastics to obtain high-quality liquid fuel, and results show that the chain length of hydrocarbon products of polyolefins increases with pore size of zeolite increasing

Yulong You contributed to the work as the first author.

✉ Xiumin Jiang
xiuminjiang@sjtu.edu.cn

[1] Institute of Thermal Energy Engineering, School of Mechanical Engineering, Shanghai Jiao Tong University, Shanghai 200240, People's Republic of China

[12–14]. Wattanapaphawong et al. [15] compared the product distribution of aliphatics with carbon number catalyzed by modified ZSM-5. Yan et al. [16] studied upgrading of gaseous tars over zeolite catalysts during coal pyrolysis and found that light hydrogen-rich products, such as H_2 and CH_4, could be served as hydrogen source for stabilization of fragments to increase volatile yield and reduce char yield during zeolite catalysis. Some researcher [6] have also reported the pyrolysis of oil shale with zeolite catalysis, which discussed product distribution and related mechanisms. Meanwhile, many researchers studied specific catalytic mechanism of zeolite based on actual industrial needs by density functional theory (DFT) calculation and molecular dynamics simulation [17–20].

Coke formation is one of the key issues in zeolite application, which is usually due to coke species deposited in the zeolites covering acid sites or blocking pores. Factors affecting coke formation in zeolites are complex and are related to characteristics of zeolites and reactants, and catalytic conditions. Therefore, many researches have been conducted to study the mechanism formation of coke in zeolite. Castaño et al. [21, 22] studied the location, properties and formation mechanism of coke in zeolites during catalytic cracking of plastics. Urata et al. [23] studied the catalytic cracking of n-hexane on HZSM-5 and found that coke is deposited on the external surface of HZSM-5 crystallites. Du et al. [24] studied the formation pathways of coke in catalytic pyrolysis of toluene, toluene with propylene, benzaldehyde and furan with ZSM-5. Shao et al. [25] studied the evolution of coke in catalytic conversion of biomass-derivated model compounds by combined in-situ DRIFTS and ex-situ approach. Williams et al. [6] reported that coke yield gradually decreases with catalytic temperature increasing from 400 to 550 °C in catalysis of ZSM-5 on shale oil, but they did not go deeper into characteristics and formation mechanism of coke.

In past years, we have conducted abundant works on thermo-chemical conversion of oil shale and kerogen [1, 2]. Shale oil is mainly composed of various aliphatics, aromatics and oxygen-containing nonhydrocarbons. Catalytic cracking, aromatization and deoxygenation of zeolites should be able to achieve the conversion of different components in shale oil. Because of product complexity of oil shale pyrolysis, further understanding catalytic mechanism is important for effective catalytic pyrolysis of oil shale pyrolysis using zeolites. Therefore, in this study, we selected two zeolites, HZSM-5 and HUSY, for catalytic pyrolysis of oil shale. We studied the product distribution of oil shale pyrolysis with zeolites in fixed bed system and Py-GCMS and analyzed the characteristics of coke in spent zeolites in fixed bed. DFT calculation was used for analyzing the adsorption of typical hydrocarbons in zeolites. Based on characteristics of oil shale pyrolysis, we analyzed the conversion of oil and gas products and coke formation in zeolites, and the effect of pore structure in zeolite, reactant characteristic and pyrolysis temperature on product distribution. These results provide a more comprehensive understanding of catalytic process, which will facilitate the development of catalytic pyrolysis technology and industrial plant design.

Experiments and calculation details

Samples

Oil shale samples from the 4th layer of Dachengzi mine located in Huadian City, China, were used in this work. The samples were crushed and sieved to a grain size of 20–40 mesh for fixed bed and 50–90 mesh for Py-GCMS. The characteristics of samples are shown in Table S1 in Supplementary Material.

Fixed bed pyrolysis

In non-catalytic experiments, 15 g dried oil shale sample was held in a stainless-steel cylindrical retort with 70 mm in internal diameter and 100 mm in height. In catalytic experiments, 15 g dried oil shale sample mechanically mixed with a certain amount of prepared catalyst was held in the above retort. Quartz wool was used to cover sample and catalyst to prevent them from being blown away by the gas flow. The details of pyrolysis system have been introduced in the authors' previous works [2]. The retort was electrically heated from room temperature to a final temperature at an average heating rate of 12 °C/min in a nitrogen atmosphere and then kept at the final temperature for 10 min. The liquid products were collected by cold traps at low temperature (~0 °C). The target gaseous products, including CH_4, C_2H_6, C_3H_8, C_4H_{10}, C_2H_4, C_3H_6, C_4H_8, CO, CO_2 and H_2, were continuously measured by GASMET DX-4000 FTIR gas analyzer and MRU Vario Plus gas analyzer. After each experiment, liquid product and shale char were collected and weighted, respectively.

Collective liquid product were separated into oil and water. Then oil was analyzed by gas chromatography–mass spectrometry experiments in a GC–MS instrument with the model of Agilent 7890A GC-5975C MS. A DB-5 chromatographic column (30 m × 0.25 mm × 0.25 μm) was used. A high purity helium of 99.999% was chosen as the carrier gas with a constant flow rate of 1 mL min^{-1}. The column was initially kept at 50 °C for 3 min and then heated to 300 °C at a heating rate of 10 °C min^{-1}. The temperature was kept for 10 min, and later 1 μL oil was injected with a gas to sample ratio 10:1. Mass spectra were recorded under electron ionization with the energy of 70 eV and the m/z range of 33–500 au. The quadrupole temperature and the ion source temperature were 150 °C and 230 °C, respectively. The interface

temperature was 280 °C. The results were identified by the NIST2014 mass spectrum library.

Py-GCMS

Fast pyrolysis experiments were conducted on a system combined with Frontier EGA/PY-3030D pyrolyzer, Agilent 7890A GC and 5975C MS. In each test, 1 mg sample was pyrolyzed under Ar atmosphere (1.0 mL min^{-1}). In the gas chromatograph, Ar was used as the carrier gas and the split ratio was 50:1. The column was DB-5 ms chromatograph column (30 m × 0.25 mm × 0.25 μm). The column was programmed from 50 to 310 °C at 5 °C min^{-1} and held for 8 min. Mass spectra were recorded under electron ionization with the energy of 70 eV and the m z^{-1} 1 range of 20–550 au. The quadrupole temperature and the ion source temperature were 150 °C and 230 °C, respectively. The interface temperature was 300 °C. The results were identified by the NIST2011 mass spectrum library.

Catalyst characteristics

The zeolite catalysts of HZSM-5 ($SiO_2/Al_2O_3 = 50$) and HUSY ($SiO_2/Al_2O_3 = 11$) used in this work were obtained from the Catalyst Plant of Nankai University. The catalysts were sieved to a particle size of 20–40 mesh for fixed bed and 50–90 mesh for Py-GCMS, and calcined in muffle furnace at a temperature of 550 °C for 5 h before use. N_2 adsorption–desorption was carried in Micromeritic ASAP 2010. Micropore volume was calculated using the t-plot method. Total pore volume of pores was determined from the adsorbed volume at P/Po = 0.95. Mesopore volume was determined from total pore volume minus micropore volume. Results are shown in Table S2 in Supplementary Material.

Analysis methods are briefly described as follows. Spent zeolite in catalytic slow pyrolysis was separated from shale char by sieving. Coke yield was obtained by calcination of spent zeolite at 850 °C in a muffle furnace. Spent zeolites in catalytic slow pyrolysis with final temperature of 520 °C and oil shale to zeolite ratio of 10:1 were further analyzed as following.

Thermogravimetric analysis of spent zeolites was carried in NETZSCH STA 2500 thermal analyzer system. 10 mg spent zeolite was used per experiment in a range from ambient temperature to 900 °C at heating rate of 20 °C min^{-1}. Gas flow of high purity air with 50 mL min^{-1} was used as the atmosphere.

Solid-state ^{13}C nuclear magnetic resonance (NMR) spectroscopy of spent zeolites was performed on a Bruker Advance 400 MHz NMR spectrometer. Cross-polarization (CP) and magic angle spinning (MAS) techniques were applied to improve signal-to-noise ratios for solid hydrocarbons. Meanwhile, total sideband suppression (TOSS) technique was employed to remove the sidebands. To obtain the quantitative information of different carbon types in spent zeolites, the ^{13}C NMR spectrums were fitted according to the chemical shifts of peaks and related structural parameters were calculated according to references [1, 26].

For analysis of soluble coke, 100 mg spent zeolite for coke analysis is dissolved in 4 mL CH_2Cl_2 for 1 h. The mixture was centrifuged and then collected the supernatant liquid called external soluble coke. Remaining mixture was filtered and solid residue was collected. After drying, the residue was dissolved in 20 mL 40% HF solution for 1 h, and then 4 mL CH_2Cl_2 was added to the solution. After stratification, subnatant liquid was collected and called internal soluble coke. These two types of soluble coke were analyzed by GCMS as mentioned above.

DFT calculation

Structures of HZSM-5 and HUSY are taken from references [27, 28]. According to research needs, we have established 8 T, 46 T and 68 T HZSM-5 cluster model, and 8 T, 54 T and 68 T HUSY cluster model. For HZSM-5, Si atom located at T12 position is replaced by Al atom, and a proton H is added at the O24 position to balance the charge forming a Brønsted acid; for HUSY, Si atom located at T2 position is replaced by Al atom, and a charge-balanced proton H is also added at the O1 position to form a Brønsted acid [16]. H atom is used to compensate for the dangling bonds in the cluster model intercepted from zeolite structure. The orientation of these H atoms is consistent with the original bond, and the length of Si–H bond is set to 1.47 Å [17]. Details of display and description of these cluster models are shown in the Supplementary Material.

ONIOM method was used and used models were divided into high layer and low layer. As shown in Figures S1(c–f) and S2 in Supplementary Material, the parts shown in the ball-stick form in HZSM-5 (14 T) and HUSY (16 T) as well as the adsorbed molecules serve as the high layer. In order to better describe the weak interaction and the van der Waals force in long-range action between adsorbed molecule and zeolite and, high-layer region was calculated at the level of ωB97XD/6–31 + G(d,p). The rest of model is used as the low layer and is calculated using the PM6 method. In the calculation, 5 T [(SiO)3Al(OH)Si] in high layer and adsorbed molecule are completely relaxed during structure optimization, and the rest are fixed on the original position. Single-point energy calculation of the overall optimized structure is calculated at the ωB97XD/6–31 + G(d,p) level. 8 T model is directly calculated at the ωB97XD/6–31 + G(d,p) level. All adsorption energy is obtained at 500°C. The isosurface plots of the reduced density gradient (RDG) for some adsorption

states in zeolites are obtained by calculating the RDG functions (RDG(r) = 1/(2(3p2)(1/3))|Dq(r)|/q(r)(4/3)) with Multiwfn software [29] and are visualized using VMD software [30]. All DFT calculations were performed with the Gaussian 16 package [31].

Results and discussion

Catalytic pyrolysis in fixed bed

Figure 1a shows the product distribution of oil shale slow pyrolysis with different catalyst addition at 520 °C. Increasing catalyst addition causes reduction of oil yield and increase in gas, H_2O and coke yield. Under the same amount of catalyst addition, HZSM-5 has higher gas yield, while HUSY has higher oil and coke yield. Char yield of catalytic pyrolysis at the oil shale to zeolite ratio of 10:1 and 6:1 is lower than that of non-catalytic pyrolysis. These results indicate that a certain amount of zeolites promote oil cracking to generate gas and enhance decomposition of oil shale to reduce char yield. However, formation of coke increases total yield of solid products, and it is more remarkable in HUSY. Table 1 shows the mass fraction of coke in spent zeolites. As zeolite addition increases, mass fraction of coke in spent HZSM-5 decreases, while that in spent HUSY increases and reaches a maximum at the ratio of 10:1. It indicates that coke formation in HUSY is more intense than that in HZSM-5. Figure 1b shows the product distribution of oil shale slow pyrolysis at 490 °C. In non-catalytic pyrolysis, increasing temperature promotes decomposition of oil shale to reduce char yield and increase yields of oil, gas and H_2O. In catalytic pyrolysis, oil yield of catalytic pyrolysis with HZSM-5 and with HUSY, respectively, increases and decreases as temperature rises. Besides, increasing temperature causes reduction of coke yield of catalytic pyrolysis with HZSM-5 and mass fraction of coke in spent HZSM-5, while increase in coke yield of catalytic pyrolysis with HUSY and proportion of coke in spent HUSY.

Table 1 Mass fraction of coke in spent zeolites (mass%)

Ratio of oil shale to zeolite	Temperature	HZSM-5	HUSY
20:1	520 °C	7.83	16.08
15:1		5.96	17.52
10:1		4.78	20.36
6:1		2.88	18.25
10:1	490 °C	6.72	15.49

Distribution of oil products

Figure 2 and Table 2 show the distribution of identified products in shale oil of slow pyrolysis. Unpresented part is unidentified compounds. In non-catalytic slow pyrolysis, shale oil primarily consists of aliphatics which are basically straight hydrocarbons, and the content of alkanes is higher than that of alkenes. Aromatics are mainly benzenes and their content is relatively low. Nonhydrocarbons are mainly oxygen-containing compounds, including alcohols, ketones, aldehydes, acids, ethers and phenols and so on. As temperature rises from 490 to 520 °C, the content of alkenes increases caused by intensified secondary cracking of oil products. High temperature also promotes decomposition of oil shale and aromatization [1, 2], increasing the content of benzenes and naphthalenes. Besides, the content of nonhydrocarbons and unidentified compounds decreases with temperature increasing, which is due to decomposition of complex fraction and removal of heteroatom functional groups in oil [2].

Zeolites change the distribution of oil products. Reduction of content of aliphatics in shale oil should be due to cracking of aliphatics catalyzed by zeolite [6, 14, 15]. The content of Alkenes significantly decreases and it is more remarkable in catalytic slow pyrolysis with HZSM-5 than that with HUSY. Proportion of cyclic and branched aliphatics in total aliphatics in shale oil of catalytic slow pyrolysis with HZSM-5 is highest. Proportion of cyclic and branched aliphatics in total aliphatics in shale oil of catalytic slow

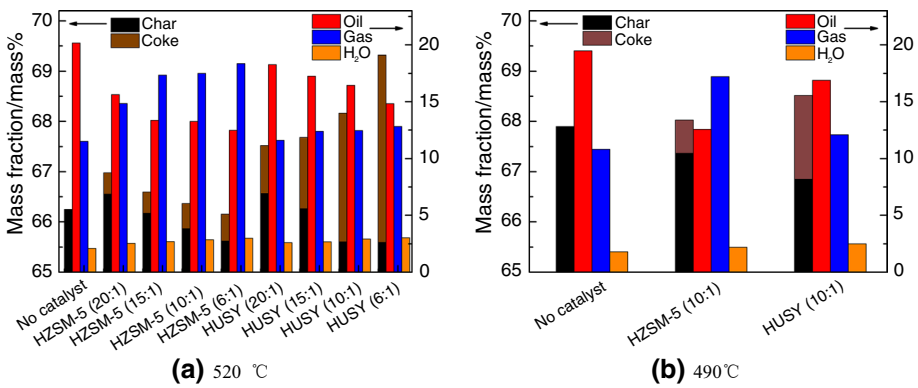

Fig. 1 Product distribution of oil shale catalytic slow pyrolysis in fixed bed

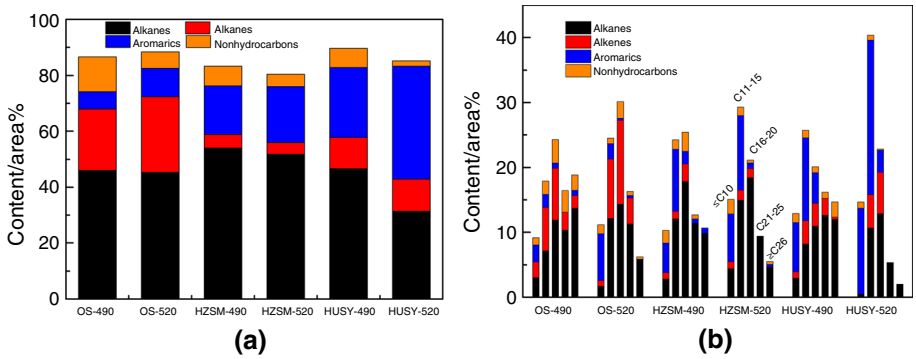

Fig. 2 Product distribution of shale oil of catalytic slow pyrolysis in fixed bed

Table 2 Product distribution of shale oils of catalytic slow pyrolysis in fixed bed (area%)

Products		OS-490	OS-520	HZSM-490	HZSM-520	HUSY-490	HUSY-520
Aliphatics	n-Alkanes	38.81	40.12	40.56	44.41	34.55	29.21
	Cycloalkanes	5.60	3.73	10.12	4.65	6.99	1.07
	Branched alkanes	1.66	1.47	3.28	2.77	5.13	0.57
	n-Alkenes	20.36	26.84	2.71	2.31	10.84	11.35
	Cycloalkenes	1.01	0.19	0.55	–	0.05	–
	Branched alkenes	0.49	–	1.61	1.79	0.19	0.17
Aromatics	Benzenes	3.89	8.25	8.31	10.55	9.32	17.83
	Biphenyls	0.05	–	0.45	0.26	1.11	1.76
	Indenes	0.74	0.33	1.64	2.74	1.09	2.16
	Naphthalenes	0.96	1.64	4.64	4.61	7.41	11.73
	Others[a]	0.62	–	2.42	1.92	6.17	6.95
Nonhydrocarbons	Oxy-aliphatic compounds[b]	10.34	4.82	1.40	0.98	4.67	0.48
	Oxy-aromatic compounds[c]	0.35	0.64	1.32	1.95	1.14	0.45
	Other[d]	1.80	0.34	4.30	1.50	0.96	0.99

[a]Other aromatics include fluorenes, phenanthrenes, anthracenes and other polycyclic aromatics

[b]Oxy-aliphatic compounds include alcohols, ketones, acids, aldehydes, esters and other compounds with oxygen and without aromatic rings

[c]Oxy-aromatic compounds include phenols and other compounds with oxygen aromatic rings

[d]Other nonhydrocarbons are compounds containing N and S

pyrolysis with HUSY is higher than that in shale oil of non-catalytic slow pyrolysis at 490 °C, while situation is reversed at 520 °C. It is reported that aliphatics will undergo isomerization and cyclization under the catalysis of zeolite in addition to catalytic cracking [12, 13, 32]. Above results indicate that HZSM-5 and HUSY differ in catalytic conversion of aliphatics. Oligomerization, cyclization, hydrogen transfer and dehydrogenation of light alkenes catalyzed by zeolite are important ways for the formation of aromatics [18, 33, 34].

For the distribution of aromatics in shale oil, HUSY has a more significant catalytic effect than HZSM-5. Compared to non-catalytic slow pyrolysis, catalytic slow pyrolysis reduces the proportion of benzenes in aromatics and increases the content of naphthalenes. Besides, HZSM-5 promotes the formation of indenes, while HUSY promotes the formation of polycyclic aromatic hydrocarbons, such as fluorenes, phenanthrenes and anthracenes. The difference in aromatics in shale oil of catalytic slow pyrolysis with two zeolites should be due to pore characteristics of zeolites [10] and more detailed discussions will be discussed in the following sections. The content of aromatics in shale oil of catalytic slow pyrolysis increases as temperature rises. Significant increase in aromatics in shale oil of catalytic slow pyrolysis with HUSY at 520 °C causes reduction of the content of aliphatics.

The content of total nonhydrocarbons and oxy-aliphatic compounds decreases under zeolite catalysis, and the effect is more significant with temperature increasing. However, the content of oxy-aromatic compounds and heteroatomic compounds relatively increases. Compounds such as alcohols, ketones, aldehydes, acids and so on have high reactivity and can be converted to hydrocarbons by deoxygenation with zeolites [7–11]. Phenols can be catalyzed to form aromatics by cracking and oligomerization, but however they

have relatively low reactivity and are easy to form coke by thermal condensation [11, 35]. Therefore, it is speculated that significant reduction of oxy-aliphatic compounds results in relative increase in the content of oxy-aromatic and heteroatomic compounds. The content of oxy-aliphatic compounds in shale oil of catalytic slow pyrolysis with HZSM-5 is lower than that with HUSY.

Zeolites promote the transfer of oil products from heavy fraction with high carbon number to light fraction with low carbon number. C16-20 products in shale oil of non-catalytic slow pyrolysis dominate, while the content of C11-15 products in shale oil of catalytic slow pyrolysis is the highest. Increase in the content of $C \leq 20$ products in shale oil of catalytic slow pyrolysis is mainly due to decrease in the content of $C \geq 21$ aliphatics and increase in the content of $C \leq 20$ aromatics, corresponding to the processes of cracking and aromatization. This catalytic effect is enhanced with temperature increasing. The content of $C \leq 20$ alkanes in shale oil of catalytic slow pyrolysis with HZSM-5 is higher, while HUSY results in lower content of $C \geq 21$ aliphatics in shale oil.

Distribution of gas products

Table 3 shows the distribution of gas products in oil shale slow pyrolysis. In non-catalytic pyrolysis, CH4 is the majority of hydrocarbon gases. Increasing temperature promotes yield of hydrocarbon gases, and increase in ratio of alkenes/alkanes reflects intensified secondary cracking [1, 2]. Yield of hydrocarbon gases significantly increases in catalytic pyrolysis. HZSM-5 has a higher yield of hydrocarbon gases than HUSY. HZMS-5 promotes the formation of CH_4, C_3H_8 and C_3H_6, and HUSY promotes the formation of C_3H_8, C_4H_{10} and C_3H_6.

In non-catalytic pyrolysis, yields of CO_2, CO and H_2 increase as temperature raises, indicating that high temperature promotes removal of oxygen and secondary reactions. Compared to non-catalytic pyrolysis, yields of CO_2 and CO have no obvious change while H_2O yield increases in catalytic pyrolysis. It reflects that oxygen in nonhydrocarbons in shale oil is mainly transferred to H_2O with zeolite catalysis. H_2 yields in catalysis slow pyrolysis with two zeolites and CH_4 yield in catalysis slow pyrolysis with HUSY decrease compared to non-catalytic pyrolysis. Some studies [12, 16] have found that hydrogen-rich light compounds provide free radicals to stabilize molecular fragments in zeolite catalysis. Thus, it is speculated that in pyrolysis of oil shale, abundant light hydrogen-rich compounds generated from catalytic reactions, including H_2 and CH_4, are converted by reacting with char to reduce the char yield.

Py-GCMS

Figure 3 and Table 4 show the distribution of identified volatile products in Py-GCMS. It could be seen that the distribution of oil products in fast and slow pyrolysis has some similarities. The content of identified volatiles in catalytic fast pyrolysis with HZSM-5 and HUSY are close. However, with temperature raising, the content of alkanes and alkenes increases while the content of aromatics and nonhydrocarbons decreases in catalytic fast pyrolysis with HZSM-5; the content of aromatics significantly increases in catalytic fast pyrolysis with HUSY. In $C \geq 6$ oil products, HZSM-5 increases the proportion of cyclic and branched aliphatics in total aliphatics, which is different with HUSY. Compared to catalytic slow pyrolysis, HZSM-5 increases the proportion of benzenes in aromatics in catalytic fast pyrolysis. Distribution of types of aromatics in oil products from catalytic fast and slow pyrolysis with HUSY are similar. Catalysis effect of zeolites on nonhydrocarbons in fast pyrolysis is also primarily directed to oxy-aliphatic compounds.

In catalytic fast pyrolysis with HZSM-5, the content of $C \leq 10$ volatiles is highest and the content of hydrocarbons significantly decreases with the increase in carbon number. In $C \geq 6$ oil products, the content of $C \leq 20$ alkanes in catalytic fast pyrolysis with HZSM-5 is higher than that with HUSY, which is consistent with catalytic slow pyrolysis. In catalytic fast pyrolysis with HZSM-5, alkenes dominantly

Table 3 Distribution of gas products of shale oils of catalytic slow pyrolysis in fixed bed (mL g^{-1})

Products	OS-490	OS-520	HZSM-490	HZSM-520	HUSY-490	HUSY-520
CH_4	34.02	38.28	63.01	71.76	11.01	15.32
C_2H_6	4.05	4.45	5.64	5.90	0.81	1.10
C_3H_8	8.21	8.80	11.18	12.49	13.73	13.18
C_4H_{10}	2.34	2.76	6.40	4.88	7.42	8.19
C_2H_4	2.14	2.61	5.44	4.40	3.29	3.12
C_3H_6	5.15	5.73	11.66	15.30	8.59	8.92
C_4H_8	0.50	0.74	1.70	1.41	2.15	2.07
CO_2	14.89	15.76	16.68	17.93	13.20	13.98
CO	5.99	7.66	6.67	6.23	6.01	6.79
H_2	4.46	9.62	2.85	5.43	4.49	5.88

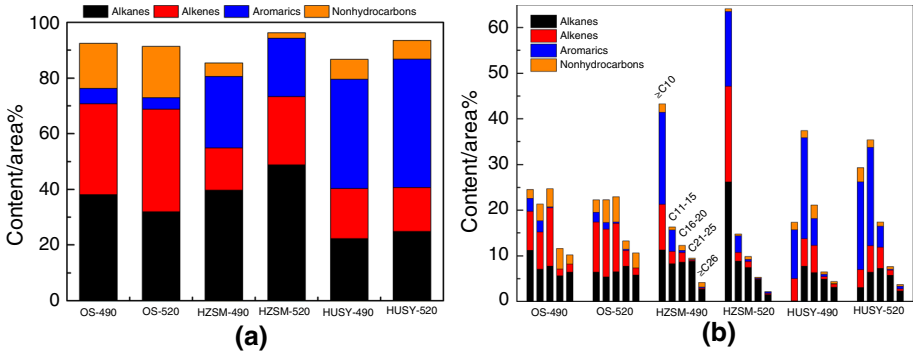

Fig. 3 Product distribution of shale oil of catalytic fast pyrolysis in Py-GCMS

Table 4 Product distribution of shale oils of catalytic fast pyrolysis in Py-GCMS (area%)

Products		OS-490	OS-520	HZSM-490	HZSM-520	HUSY-490	HUSY-520
Aliphatics	n-Alkanes	28.74	24.47	29.69	24.32	18.16	22.41
	Cycloalkanes	8.44	5.94	8.10	22.73	3.10	1.02
	Branched alkanes	0.94	1.52	1.92	1.79	0.98	1.40
	n-Alkenes	30.76	30.83	6.64	15.73	18.08	12.75
	Cycloalkenes	0.97	0.76	2.42	3.52	–	0.88
	Branched alkenes	0.92	5.28	6.08	5.27	–	2.22
Aromatics	Benzenes	3.34	2.81	21.74	16.99	13.76	20.39
	Biphenyls	0.07	–	–	–	3.56	3.17
	Indenes	0.90	0.98	1.57	1.54	3.40	3.84
	Naphthalenes	1.23	0.33	2.07	1.91	11.50	12.10
	Others[a]	–	0.06	0.40	0.50	7.06	6.67
Nonhydrocarbons	Oxy-aliphatic compounds[b]	10.38	9.36	2.03	0.71	2.92	3.59
	Oxy-aromatic compounds[c]	2.25	3.63	1.53	0.87	0.32	1.45
	Other[d]	3.49	5.35	1.29	0.48	3.90	1.61

a, b, c, d have the same definition as shown in Table 2

concentrate in C ≤ 5 volatiles and C > 10 alkenes are much less. Differently, the content of C11-20 alkenes in catalytic fast pyrolysis with HUSY is still high. The difference in carbon number distribution of aliphatics should be related to pore structure of HZSM-5 and HUSY [13]. Besides, more aromatics concentrate in C ≤ 10 volatiles catalyzed by HZSM-5 in fast pyrolysis compared to slow pyrolysis. As temperature rises from 490 to 520 °C, the content of C ≥ 21 aliphatics further decreases and the content of C ≤ 10 aliphatics significantly increases in catalytic fast pyrolysis with HZSM-5, while the content of C ≤ 10 aromatics increases in catalytic fast pyrolysis with HUSY. These results indicate that increasing temperature promotes cracking in HZSM-5 catalysis and aromatization in HUSY catalysis.

Coke characteristics

Figure 4 shows TG analysis of spent HZSM-5 and HUSY. Mass loss of spent zeolites is located in the range of 300–800 °C, which indicates that coke is complex multi-component substance. It is considered that mass loss below 450 °C is due to coke partly containing aliphatic carbons, and mass loss above 500 °C is related to coke which has high aromaticity [21, 36]. By comparison, TG curve of spent HZSM-5 is gentler, while TG curve of spent USY is closer to high-temperature zone. It means that coke in HUSY has more compact aromatic structure.

Table 5 is the ^{13}C NMR results of spent zeolites corresponding to Figure S3 in Supplementary Material. It shows that spent HUSY has high aromaticity while spent HZSM-5 contains more aliphatic carbon. Aliphatic carbon is mainly methyls (14–16 ppm and 16–22 ppm), and spent HZSM-5 has more methylenes (22–40 ppm). This causes the difference in aliphatic chain length between coke in two zeolites. Compared to spent HZSM-5, spent HUSY has more aromatic bridgehead carbon (130–135 ppm) and its aromatic cluster has larger size by calculation, which reflects a higher degree of condensation. These results are consistent with TG analysis above.

Figure 5a shows the GCMS results of soluble coke in spent HZSM-5 and HUSY. Soluble coke mainly contains alkanes, aromatics and nonhydrocarbons. In internal soluble

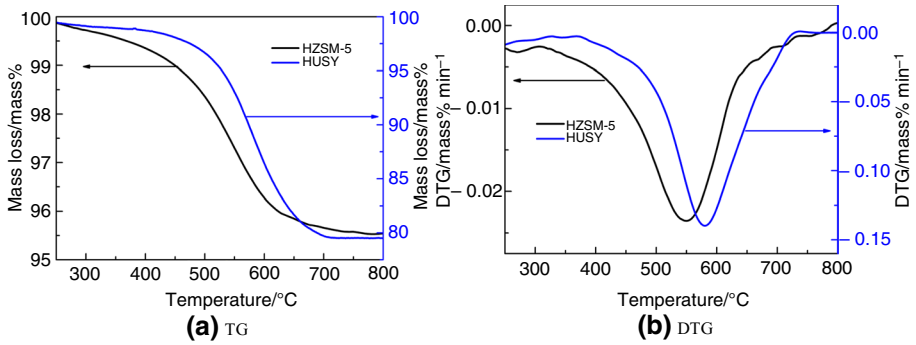

Fig. 4 Thermogravimetric analysis of spent zeolites from catalytic slow pyrolysis at 520 °C in fixed bed

Table 5 Structural parameters from ^{13}C NMR results of spent zeolites

	HZSM-5	HUSY
Content of aliphatic carbon (0–90 ppm, mol%)	42.28	25.24
Content of aromatic carbon (90–220 ppm, mol%)	51.44	69.14
Average methylene chain length	2.02	0.06
Average number of carbons per aromatic cluster	6.78	8.75

coke in spent HZSM-5, the content of nonhydrocarbons and aromatics is high, aromatics are mainly distributed in C11-15, nonhydrocarbons are distributed in C ≤ 25, and C ≥ 26 alkanes have highest content in total aliphatics. Internal soluble coke in spent USY is mainly composed of alkanes which has a wide distribution of carbon number, aromatics are distributed in C16–20, and nonhydrocarbons are distributed in C ≤ 21. External soluble coke in spent HZSM-5 mainly contains aliphatics, especially C ≥ 21 aliphatics. External soluble coke in spent HUSY is mainly composed of C11–25 aromatics and nonhydrocarbons, and there are no C ≥ 26 compounds.

Some researchers have done works on the sources of aliphatics in coke. Villegas et al. [32] studied catalytic cleavage of n-butane on ZSM-5 and H-Beta and found that coke in zeolites is mainly soluble coke which is mainly composed of long linear alkenes formed by consecutive oligomerization of n-butane. However, our results show the low content of alkenes in soluble coke in zeolites. It indicates that aliphatics enter to zeolites, alkenes are fast consumed while alkanes react slowly and then are trapped to form coke. Meanwhile, it is reported [21, 23] that aliphatics will be deposited in the surface of ZSM-5 during catalytic cracking of aliphatics with ZSM-5, which should be the reason for high content of aliphatics in external soluble coke in spent HZSM-5. By contrast, the content of aliphatics in external coke in spent HUSY is low. High content of aliphatics in internal coke in spent HUSY is not consistent with NMR results of spent HUSY, which indicates that the proportion of internal soluble coke accounted for total coke is small. Besides, carbon distribution of aliphatics in internal coke in spent HUSY is similar to shale oil. These results reflect sufficient diffusion of aliphatics in HUSY. As shown in Fig. 5b, alkanes in internal soluble coke in spent zeolites are mainly straight alkanes. External soluble coke in spent HUSY basically has no cyclic and branched aliphatics, while the content of cyclic and branched aliphatics in external soluble coke in spent HZSM-5 is relatively high.

Table 6 shows the typical aromatics and nonhydrocarbons in internal soluble coke in spent zeolites. It was found that Phenol, 2,2′-methylenebis[6-(1,1-dimethylethyl)-4-methyl-, o-Terphenyl and Benzo[b]fluoranthene do not exist in shale oil of non-catalytic slow pyrolysis. It indicates that these aromatics and oxy-aromatic compounds in internal soluble coke are formed during catalytic pyrolysis of oil shale. Aromatics formed from decomposition of oil shale and aromatization of alkenes could be converted to polycyclic aromatics and eventually coke by alkylation and hydrogen transfer [24]. Shao et al. [25] found that same or similar coke species as

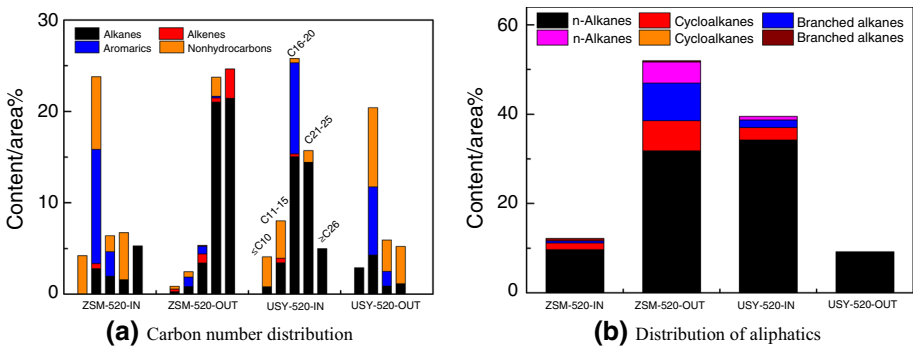

Fig. 5 Component distribution of soluble coke in spent zeolites from catalytic slow pyrolysis at 520 °C in fixed bed

Table 6 Typical aromatics and oxy-aromatic species in internal soluble coke in spent zeolites (area%)

Species	HZSM-5	HUSY
Phenol, 3-methyl-	3.21	–
Benzaldehyde, 2,4-dimethyl-	1.02	–
Benzene, (1-ethylpropyl)-	9.03	–
Benzaldehyde, 4-propyl-	–	2.89
2,4-Di-tert-butylphenol	7.95	2.61
Naphthalene, 2,3,6-trimethyl-	1.01	–
Anthracene, 9-methyl-	1.73	–
Pyrene	–	1.86
Pyrene, 1-methyl-	0.91	3.86
Phenol, 2,2'-methylenebis[6-(1,1-dimethylethyl)-4-methyl-	5.17	1.28
o-Terphenyl	–	1.6
Benzo[b]fluoranthene	–	0.83

benzaldehyde, 2,4-dimethyl-, 2,4-di-tert-butylphenol and phenol, 2,2'-methylenebis[6-(1,1-dimethylethyl)-4-methyl- in Table 6 could be formed during catalytic pyrolysis of light oxygen-containing compounds, which means that oxygen-containing nonhydrocarbons could form coke species as phenols and benzaldehydes. Phenols will convert to polycyclic aromatics by thermal condensation because of low activity [35], tolualdehydes will form coke by deoxygenation, polymerization and condensation [24]. It could be found that polycyclic aromatics are important precursors for the conversion of various compounds containing aromatic rings into coke. Compared to spent HZSM-5, polycyclic aromatics in internal soluble coke in spent HUSY have larger sizes, which is consistent with distribution of shale oil of catalytic pyrolysis with two zeolites.

Adsorption of typical hydrocarbons on zeolites during catalytic pyrolysis

Adsorption is an important process as the first step in catalytic reactions. Figure 6 shows the adsorption energies of hydrocarbons on 46 T HZSM-5 and 54 T HUSY. High adsorption energy means that strong interaction between molecules and zeolites. Adsorption and reaction of reactants on zeolites are usually considered to be affected by Brønsted acid and pore confinement [10, 19]. Adsorption energy is calculated by subtracting energy of zeolite and energy of molecule from total energy of molecule adsorbed zeolite. Adsorption on 8 T model mainly results from Brønsted acid, and thus calculated adsorption energy from 8 T model is called E_{acid}. Adsorption energy caused by pore confinement could be calculated by [19]

$$E_{confinement} = E_{ads} - E_{acid}$$

where E_{ads} is total adsorption energy.

Because of stronger adsorption effect of Brønsted acid, adsorption energy of 3-hexene on zeolites is the largest. There are several differences between HZSM-5 and HUSY. Pore confinement of HZSM-5 has a greater contribution to the adsorption of hydrocarbons on zeolites, while Brønsted acid of HUSY has a greater contribution to the adsorption of hydrocarbons on zeolites. In both zeolites, adsorption energy of benzene by Brønsted acid is higher than that of alkanes. However, adsorption energy of alkanes by pore confinement is significantly higher than that of benzene in HZSM-5, while adsorption energy of alkanes and benzene by pore confinement is similar in HUSY. It results in higher adsorption energy of alkanes than that of benzene in HZSM-5. In addition, in HZSM-5, adsorption energy of n-hexane by pore confinement is higher than that of 3-methylpentane, which is the reason for the difference in adsorption energy of two alkanes.

Figure 7 shows the results of RDG analysis of adsorption states of hydrocarbons on HZSM-5 and HUSY. The RDG isosurface reflects the interactions existing in the system. Table 7 gives the parameters of adsorption states. In HZSM-5, alkanes basically enter sinusoidal channel. The Brønsted acid, respectively, interacts with the C–C bond of n-hexane and the tertiary carbon of 3-methylpentane. The length change of O–H bond in zeolites is relatively small. Compared with n-hexane, 3-methylpentane has a larger size in the direction of sinusoidal channel and occupies more

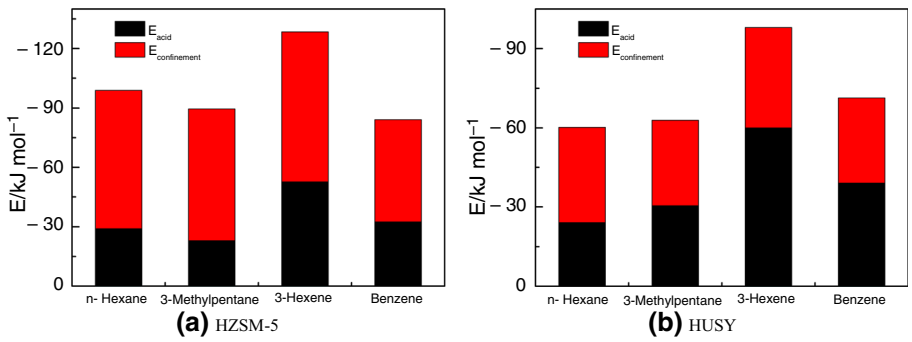

Fig. 6 Calculated adsorption energy of hydrocarbons on zeolites

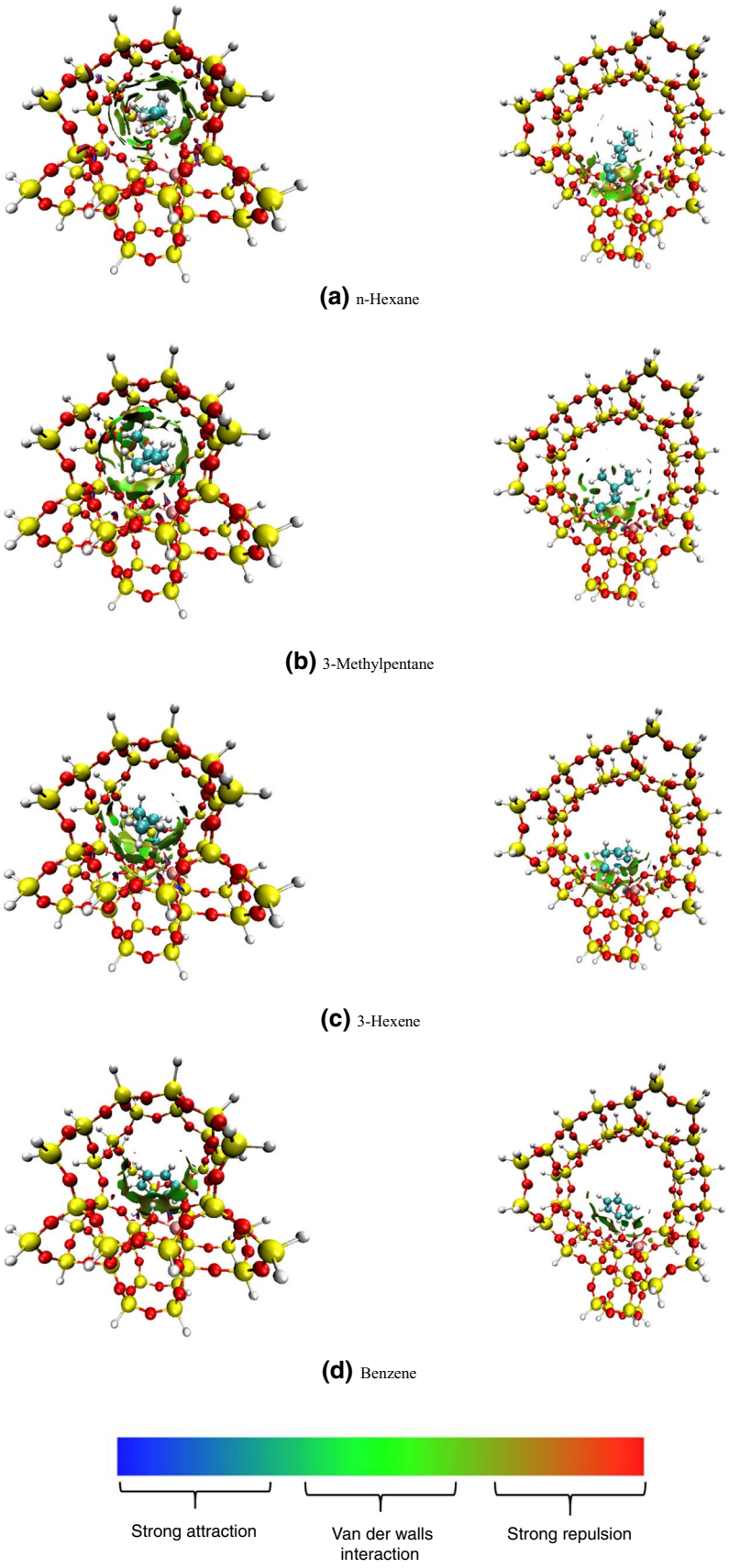

Fig. 7 Isosurface plots of the reduced density gradient (s = 0.500 a.u.) for optimized adsorption states of hydrocarbons on 46 T HZSM-5 (left) and 54 T HUSY (right)

Table 7 Structural parameters of optimized adsorption states of hydrocarbons on zeolites

	46 T HZSM-5				54 T HUSY			
	Not adsorbed		Adsorbed		Not adsorbed		Adsorbed	
	O–H	C–C	O–H	C–C	O–H	C–C	O–H	C–C
n-Hexane	0.965	1.529	0.969	1.529	0.965	1.529	0.972	1.531
3-Methylpentane		1.537	0.970	1.537		1.537	0.973	1.538
3-Hexene		1.334	0.992	1.340		1.334	0.999	1.342
Benzene		1.394	0.974	1.394		1.394	0.980	1.399

C–C represents the distance between two C atoms in adsorbed hydrocarbons closest to Brønsted acid

space. Sinusoidal channel in HZSM-5 has a stronger stabilizing effect on the adsorption of n-hexane, while the existence of branched chain leads to a greater range of repulsion between 3-methylpentane and sinusoidal channel making in C–C bond shorter in the branched chain. Alkanes mainly interact with Brønsted acid, and the down, left and right side of channel as shown in HUSY. In this large space, 3-methylpentane with a branched chain is more stabilized by pore of HUSY, and thus its adsorption energy is slightly higher than that of n-hexane. Therefore, n-hexane and 3-methylpentane show different competitiveness for Brønsted acid in two zeolites. It was reported that diffusion of hydrocarbons in zeolites is affected by configuration of hydrocarbons and pore structure of zeolite [10, 20]. The above reasons make HZSM-5 and HUSY show different shape-selective capability for straight and branched alkanes, which accounts for the different proportion of cyclic and branched aliphatics in total aliphatics in shale oil from catalytic slow pyrolysis.

The interaction between C=C bond of 3-hexene and Brønsted acid is strong, and a π-complex is formed. Compared to other hydrocarbons, length change of O–H bond and C=C bond during adsorption of 3-hexene is most noticeable. It indicates that alkenes are easier to access Brønsted acid and consumed through cracking and aromatization, resulting in significant reduction in the alkene content in catalytic products. 3-Hexene mainly interacts with the down, left and right side of channel as shown. Besides, the interaction between pore of HZSM-5 and 3-hexene is more significant than HUSY. Benzene is adsorbed in zeolites through the interaction between π-bond and Brønsted acid. Channel size of HZSM-5 is relatively small, and thus benzene is located at the junction of sinusoidal and straight channel. HUSY has a larger pore size, and benzene is located in its channel. The C–C bond of benzene is basically unchanged in HZSM-5 while slightly increases in HUSY.

Figure 8 shows the adsorption of n-dodecane in HZSM-5 and HUSY. In 68 T HZSM-5, n-dodecane deforms and occupies entire sinusoidal channel and some part space of straight channel because of its large size. In 90 T HUSY, n-dodecane still maintains approximately straight configuration, and pore of HUSY still has more free space. It could be speculated that long-chain aliphatics are tended to deposit inside the sinusoidal channel and thus hinder the diffusion of other molecules, while HUSY has an advantage in the diffusion of large-size molecules.

Adsorption of polycyclic aromatics has also been studied as shown in Figure S4 in Supplementary Material. Two typical aromatics in internal soluble coke in spent zeolites discussed above are studied. 1-Methylpyrene is located at the intersection of sinusoidal and straight channel in 68 T

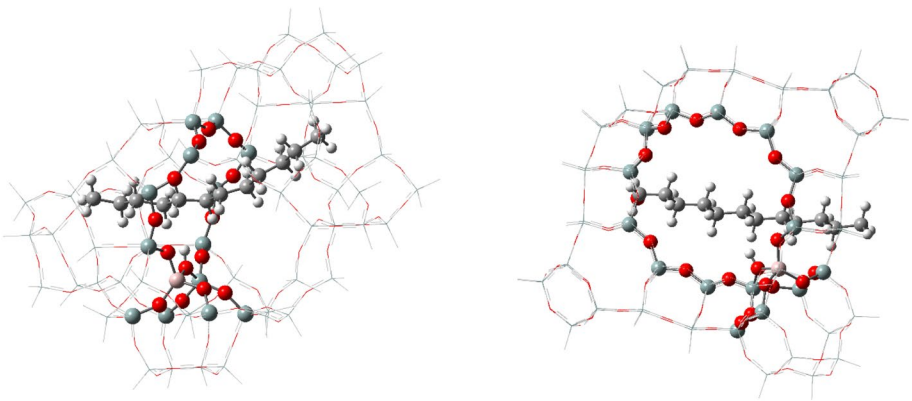

Fig. 8 Optimized adsorption states of n-dodecane on zeolites

(a) 68T HZSM-5 **(b)** 90T HUSY

HZSM-5. Due to its large size, deposit of 1-methylpyrene at this location would hinder the diffusion of others in sinusoidal and straight channel. In 90 T HUSY, 1-methylpyrene could entirely enter the 12-ring channel, and larger polycyclic aromatic, Benzo[b]fluoranthene could also form. It could be seen that pore in HUSY provides more space for growth of polycyclic aromatics than that in HZSM-5.

Catalytic mechanism of zeolite during oil shale pyrolysis

Oil shale is thermally decomposed to form primary volatiles [1, 2], which are in contact with the zeolite and undergo a series of catalytic reactions. As discussed above, catalytic pyrolysis of oil shale with zeolite could be summarized as shown in Fig. 9. Various aliphatics crack to form shorter aliphatics and hydrocarbon gases [6, 14, 15]. Cracking of aliphatics should be one of important processes in catalytic pyrolysis of oil shale, which converts long-chain aliphatics to short chain aliphatics. Meanwhile, there could also be conversion of straight aliphatics to cyclic and branched aliphatics by cyclization and isomerization, and conversion of cyclic and branched aliphatics to aromatics by aromatization [12, 13, 32]. Light alkenes are converted to aromatics by aromatization [18, 33]. Deoxygenation of oxy-aliphatic compounds and cracking and oligomerization of oxy-aromatic compounds by zeolite catalysis convert nonhydrocarbons to hydrocarbons, and the former is more significant [7–11]. Cracking of aliphatics will produce abundant H and light hydrogen-rich compounds which is in favor of reduction of char yield. Meanwhile, various volatiles also convert to coke through different pathways. Aromatic carbon accounts for larger proportion in total coke compared to aliphatic carbon, and polycyclic aromatics are important precursors and compositions of coke.

Catalytic cracking decreases the content of long-chain aliphatics, but also causes the conversion of shale oil to gas products. Aromatization could transfer light alkenes to light aromatics, but also result in formation of polycyclic aromatics and coke. In comparison, catalytic pyrolysis with HZSM-5 has higher yield of hydrocarbon gases, less content of alkenes in shale oil and lower coke yield, while catalytic pyrolysis with HUSY has higher oil yield and more aromatics in shale oil. These differences are mainly caused by zeolite characteristics and pyrolysis conditions.

There are several differences between HZSM-5 and HUSY. Two zeolites have different pore structures and sizes. Compared with HUSY, HZSM-5 has greater steric

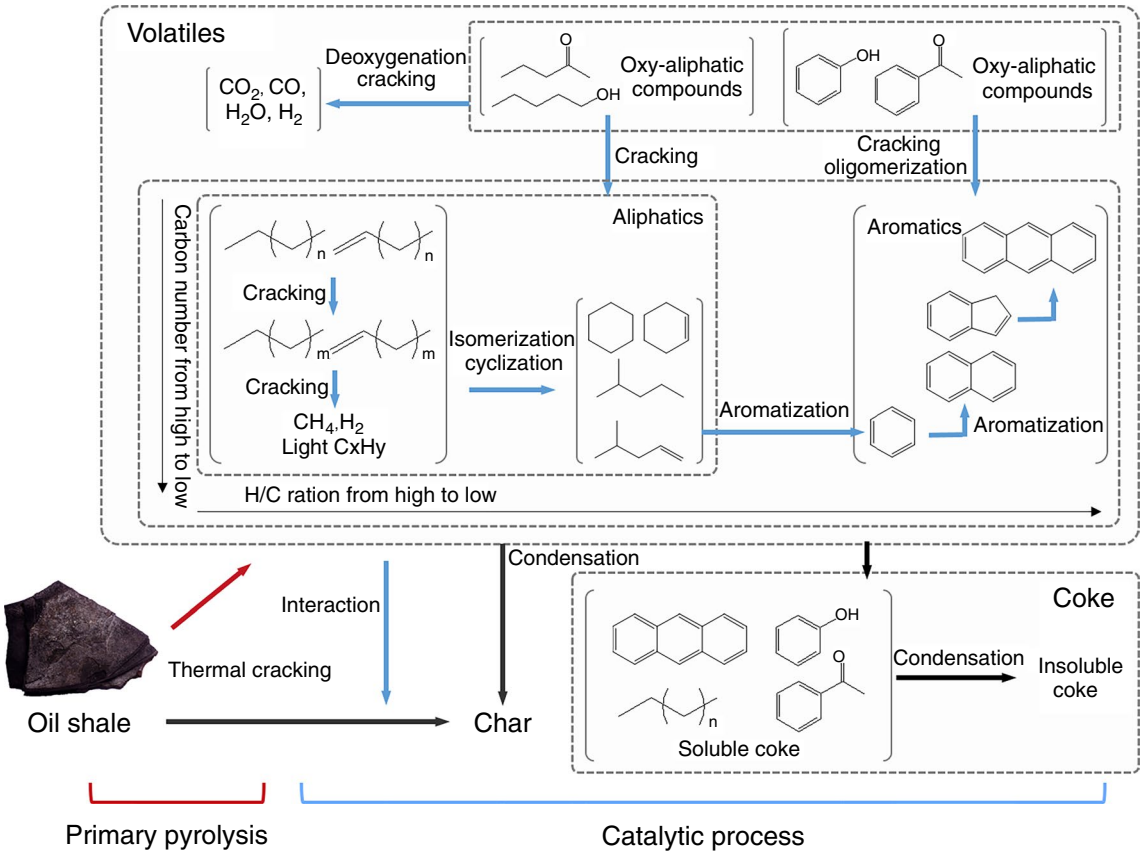

Fig. 9 Scheme of oil shale catalytic pyrolysis with zeolite

hindrance. Yuan et al. showed that straight-chain alkanes have similar diffusion energy barriers in the straight pores of MFI and FAU, while the diffusion energy barriers of branched and cyclic alkanes and macromolecular aromatics in FAU are much lower than those in MFI [20]. In addition, HZSM-5 usually has strong and weak acid sites while acidity of HUSY is weaker. Strong acid sites are more effective than weak acid sites in catalyzing hydrocarbon cracking [13]. Combining experiment results and adsorption of DFT calculations, we can analyze as follows.

Zeolite characteristics affect the conversion of oil and gas products. DFT calculations show that interaction between alkene and Brønsted acid is strongest, making alkenes highly competitive for catalytic sites in zeolites. Thus, zeolites show good catalytic ability to reduce alkenes in shale oil. HZSM-5 has a small-size pore for better shape-selective catalysis. Adsorption calculations show that straight alkanes are more likely to occupy acid site inside HZSM-5 than branched alkanes. This shape-selective capability should be the main reason accounting for the increased proportion of cyclic and branched aliphatics in total aliphatics in shale oil from catalytic pyrolysis with HZSM-5. Meanwhile, HZSM-5 also limits the formation of polycyclic aromatics. DFT calculations imply that large-size pore in HUSY is in favor of the diffusion of reactants, which could realize the catalysis on large-size fraction and thus increases the content of hydrocarbons in shale oil, but also cause the formation of polycyclic aromatics. Some researchers [13] reported strong acid sites and small pores contribute to the formation of light hydrocarbons. HZSM-5 is more effective in catalytic cracking of volatile products, thereby significantly reducing alkene content in shale oil and concentrating alkanes in low-carbon oil products. Benzene is more competitive than hexane in HUSY, which should be the reason for stronger catalytic aromatization of HUSY.

Besides, zeolite characteristics also affect formation and characteristics of coke. Small-size pore in HZSM-5 blocks the diffusion of macromolecules. Cyclic and branched aliphatics might be blocked outside of HZSM-5, resulting in high proportion of cyclic and branched aliphatics in external soluble coke in spent HZSM-5. Deposition of long-chain aliphatics inside and outside of HZSM-5 should also be due to large steric hindrance. These deposited aliphatics cause higher content of aliphatic carbon in spent HZSM-5 as shown in NMR analysis. Therefore, coke formation in HZSM-5 should be seen as combination of growth of coke precursors in pores and deposition of long-chain compounds inside and outside of zeolite. DFT calculations indicate that large-size pore in HUSY provides more space for growth of aromatics. Castaño et al. [22] found that bimolecular reactions (such as hydrogen transfer and oligomerization) and condensation are enhanced as pore size increases. It causes high content of polycyclic aromatics in shale oil and coke yield, and high condensed aromatic structure in spent HUSY. Thus, growth of aromatics could be seen as the main reason for coke formation in HUSY.

Temperature also has different effects on various catalytic processes and conversion of oil, gas and solid products. Increasing temperature significantly promotes catalytic cracking of HZSM-5, which might reduce the blockage of long-chain aliphatics in HZSM-5 and thus reduce coke yield. Meanwhile, enhanced aromatization also promotes the conversion of hydrocarbon gases to oil products and increases oil yield. For HUSY, aromatization is obviously enhanced by increasing temperature, which results in increase in the content of polycyclic aromatics in shale oil and coke yield and reduction of oil yield. Besides, compared to catalytic slow pyrolysis, catalytic fast pyrolysis has higher content of $C \leq 10$ products in shale oil.

These results could provide some useful information for catalytic pyrolysis of oil shale. The expected catalytic process is that aliphatics in shale oil are selectively concentrated in light fraction without excessively cracking, and meanwhile an appropriate amount of light aromatics form to further improve the content of light fraction in shale oil. Therefore, Enhancing or inhibiting specific catalytic process by adjusting zeolite properties and pyrolysis condition for obtaining target products could be the key issue in future research.

Conclusions

In current work, we studied the product distribution of oil shale catalytic pyrolysis with HZSM-5 and HUSY, analyzed the coke in spent zeolites and studied the adsorption of typical hydrocarbons in zeolites by DFT calculation. Main conclusion is drawn as follows:

Catalytic pyrolysis of oil shale with zeolite could be summarized as four processes including cracking, aromatization, deoxygenation and coke formation. Catalytic cracking decreases the content of long-chain aliphatics and causes the conversion of shale oil to gas products. Aromatization could transfer light alkenes to light aromatics and result in formation of polycyclic aromatics and coke. Catalytic effect of zeolite on nonhydrocarbons is mainly deoxygenation of oxy-aliphatic compounds. Therefore, suitable cracking and aromatization of zeolite catalysis will increase the content of light fraction in shale oil. Meanwhile, various reactants will convert to coke in zeolites. Aromatic carbon accounts for larger proportion in total coke compared to aliphatic carbon, and polycyclic aromatics are important precursors and compositions of coke. In comparison, catalytic pyrolysis with HZSM-5 has higher yield of hydrocarbon gases and less content of alkenes in shale oil, while catalytic pyrolysis with HUSY has high content of aromatics in shale oil.

Catalytic pyrolysis is affected by zeolite characteristics and pyrolysis conditions. In hydrocarbons, alkenes are easier to occupy Brønsted acid, and competition between alkanes and aromatics for Brønsted acid is affected by Brønsted acid and pore structure. Small pores in HZSM-5 increase the proportion of cyclic and branched aliphatics in total aliphatics and limit the size of aromatics, but also block the diffusion of large-size compounds in HZSM-5. HUSY has larger pores, which is in favor of catalyzing heavy fraction in shale oil, but also enhances the formation of polycyclic aromatics and coke. Coke formation in HZSM-5 causes by growth of coke precursors in pores and deposition of long-chain compounds inside and outside of zeolite, while that in HUSY is mainly due to growth of coke precursors in pores. Increasing temperature significantly promotes cracking in catalytic pyrolysis with HZSM-5 and aromatization in catalytic pyrolysis with HUSY. Compared to catalytic slow pyrolysis, catalytic fast pyrolysis has higher content of $C \leq 10$ products in shale oil. These factors affect the conversion of oil, gas and solid products in catalytic pyrolysis. The study indicates optimizing zeolite characteristics and catalytic pyrolysis condition could realize directional regulation of products of oil shale.

Supplementary Information The online version contains supplementary material available at https://doi.org/10.1007/s10973-021-11138-x.

Acknowledgements This work was supported by the National Natural Science Foundation of China (Grant No. 51876122).

Author contributions All authors contributed to the study conception and design. Material preparation and data collection were performed by Yulong You, and analysis was mainly performed by Yulong You and Xiaoye Wang. The first draft of the manuscript was written by Xiaoye Wang and Yulong You and was critically revised by Xiangxin Han and Xiumin Jiang. All authors commented on previous versions of the manuscript. All authors read and approved the final manuscript.

Funding This work was supported by the National Natural Science Foundation of China (Grant No. 51876122).

Declarations

Conflict of interest The authors claim that none of the material in the paper has been published or is under consideration for publication elsewhere. The authors declare no competing financial interest.

References

1. You Y, Han X, Liu J, Jiang X. Structural characteristics and pyrolysis behaviors of huadian oil shale kerogens using solid-state 13C NMR, Py-GCMS and TG. J Therm Anal Calorim. 2018;131:1845–55.
2. Wang S, Jiang X, Han X, Tong J. Effect of retorting temperature on product yield and characteristics of non-condensable gases and shale oil obtained by retorting Huadian oil shales. Fuel Process Technol. 2014;121:9–15.
3. Hu M, Cheng Z, Zhang M, Liu M, Song L, Zhang Y, Li J. Effect of calcite, kaolinite, gypsum, and montmorillonite on huadian oil shale kerogen pyrolysis. Energy Fuel. 2014;28:1860–7.
4. Nazzal JM. The influence of grain size on the products yield and shale oil composition from the Pyrolysis of Sultani oil shale. Energy Convers Manage. 2008;49:3278–86.
5. Pan L, Dai F, Li G, Liu S. A TGA/DTA-MS investigation to the influence of process conditions on the pyrolysis of Jimsar oil shale. Energy. 2015;86:749–57.
6. Williams P, Chishti H. Two stage pyrolysis of oil shale using a zeolite catalyst. J Anal Appl Pyrolysis. 2000;55:217–34.
7. Gayubo AG, Aguayo AT, Atutxa A, Aguado R, Bilbao J. Transformation of oxygenate components of biomass pyrolysis oil on a HZSM-5 zeolite I Alcohols and phenols. Ind Eng Chem Res. 2004;43:2610–8.
8. Gayubo AG, Aguayo AT, Atutxa A, Aguado R, Olazar M, Bilbao J. Transformation of oxygenate components of biomass pyrolysis oil on a HZSM-5 zeolite. II Ind Eng Chem Res. 2004;43:2619–26.
9. Zhao Y, Yang X, Fu Z, Li R, Wu Y. Synergistic effect of catalytic co-pyrolysis of cellulose and polyethylene over HZSM-5. J Therm Anal Calorim. 2000;140:363–71.
10. Jae J, Tompsett GA, Foster AJ, Hammond KD, Auerbach SM, Lobo RF, Huber GW. Investigation into the shape selectivity of zeolite catalysts for biomass conversion. J Catal. 2011;279:257–68.
11. Wang K, Kim KH, Brown RC. Catalytic pyrolysis of individual components of lignocellulosic biomass. Green Chem. 2014;16:727–35.
12. Zhang X, Lei H, Zhu L, Qian M, Zhu X, Wu J, Chen S. Enhancement of jet fuel range alkanes from co-feeding of lignocellulosic biomass with plastics via tandem catalytic conversions. Appl Energy. 2016;173:418–30.
13. Lopez G, Artetxe M, Amutio M, Bilbao J, Olazar M. Thermochemical routes for the valorization of waste polyolefinic plastics to produce fuels and chemicals. A review Renew Sust Energy Rev. 2017;73:346–68.
14. Caldeira VPS, Santos AGD, Oliveira DS, Lima RB, Souza LD, Sibele BC. Polyethylene catalytic cracking by thermogravimetric analysis. J Therm Anal Calorim. 2017;130:1939–51.
15. Wattanapaphawong P, Reubroycharoen P, Mimuraa N, Satoa O, Yamaguchia A. Effect of carbon number on the production of propylene and ethylene by catalytic cracking of straight-chain alkanes over phosphorus-modified ZSM-5. Fuel Process Technol. 2020;202:106367.
16. Yan L, Bai Y, Liu Y, He Y, Li F. Effects of low molecular compounds in coal on the catalytic upgrading of gaseous tar. Fuel. 2018;226:316–21.
17. Maihom T, Pantu P, Tachakritikul C, Probst M, Limtrakul J. Effect of the zeolite nanocavity on the reaction mechanism of n-hexane cracking: a density functional theory study. J Phys Chem C. 2010;17:7850–6.
18. Wang S, Chen YY, Qin Z, Zhao T, Fan S, Dong M, Li J, Fan W, Wang J. Origin and evolution of the initial hydrocarbon pool intermediates in the transition period for the conversion of methanol to olefins over H-ZSM-5 zeolite. J Catal. 2019;369:382–95.
19. Fu J, Feng X, Liu Y, Yang C. Effect of pore confinement on the adsorption of mono-branched alkanes of naphtha in ZSM-5 and Y zeolites. Appl Surf Sci. 2017;423:131–8.
20. Yuan S, Liu Y, Tian H, Dai Z, Zhao Y, Zhou H, Long J. Study on Diffusion of Hydrocarbons in FAU and MFI Zeolites by Molecular Simulation and Related Experiments. China Petroleum Process Petrochem Technol. 2012;14:1–8.
21. Ibáñez M, Artetxe M, Lopez G, Elordi G, Bilbao J, Olazar M, Castaño P. Identification of the coke deposited on an HZSM-5 zeolite catalyst during the sequenced pyrolysis–cracking of HDPE. Appl Catal B Environ. 2014;148:436–45.

22. Castaño P, Elordi G, Olazar M, Aguayo AT, Pawelec B, Bilbao J. Insights into the coke deposited on HZSM-5, Hβ and HY zeolites during the cracking of polyethylene. Appl Catal B Environ. 2011;104:91–100.
23. Urata K, Furukawa S, Komatsu T. Location of coke on H-ZSM-5 zeolite formed in the cracking of n-hexane. Appl Catal A Gen. 2014;475:335–40.
24. Du S, Gamliel DP, Giotto MV, Valla JA, Bollas GM. Coke formation of model compounds relevant to pyrolysis bio-oil over ZSM-5. Appl Catal A Gen. 2016;513:67–81.
25. Shao S, Zhang H, Xiao R, Li X, Cai Y. Evolution of coke in the catalytic conversion of biomass-derivates by combined in-situ DRIFTS and ex-situ approach: Effect of functional structure. Fuel Process Technol. 2018;178:88–97.
26. Solum MS, Pugmire RJ, Grant DM. 13C solid-state NMR of Argonne premium coals. Energy Fuel. 1989;3:187–93.
27. van Koningsveld H, van Bekkum H, Jansen JC. On the location and disorder of the tetrapropylammonium (TPA) ion in zeolite ZSM-5 with improved framework accuracy. Acta Crystallogr A. 1987;B43:127–32.
28. Baur WH. On the cation and water positions in faujasite. Am Miner. 1964;49:697–704.
29. Lu T, Chen F. Multiwfn: A multifunctional wavefunction analyzer. J Comput Chem. 2012;33:580–92.
30. Humphrey W, Dalke A, Schulten K. Vmd: Visual Molecular Dynamics. J Mol Graph. 1996;14:33–8.
31. Frisch MJ, Trucks GW, Schlegel HB, et al. Gaussian 16, Revision A.03; Gaussian, Inc.: Wallingford, CT, 2016.
32. Villegas JI, Kumar N, Heikkilä T, Lehto VP, Salmi T, Murzin DY. Isomerization of n-butane to isobutane over Pt-modified Beta and ZSM-5 zeolite catalysts: Catalyst deactivation and regeneration. Chem Eng J. 2006;120:83–9.
33. Kuo Y, Almansa GA, Vreugdenhil BJ. Catalytic aromatization of ethylene in syngas from biomass to enhance economic sustainability of gas production. Appl Energy. 2018;215:21–30.
34. Wang G, Xu C, Gao J. Study of cracking FCC naphtha in a secondary riser of the FCC unit for maximum propylene production. Fuel Process Technol. 2008;89:864–73.
35. Gueudré L, Thegarid N, Burel L, Jouguet B, Meunier F, Schuurman Y, Mirodatos C. Coke chemistry under vacuum gasoil/bio-oil FCC co-processing conditions. Catal Today. 2015;257:200–12.
36. Bayraktar O, Kugler EL. Coke content of spent commercial fluid catalytic cracking (FCC) catalysts. J Therm Anal Calorim. 2003;71:867–74.